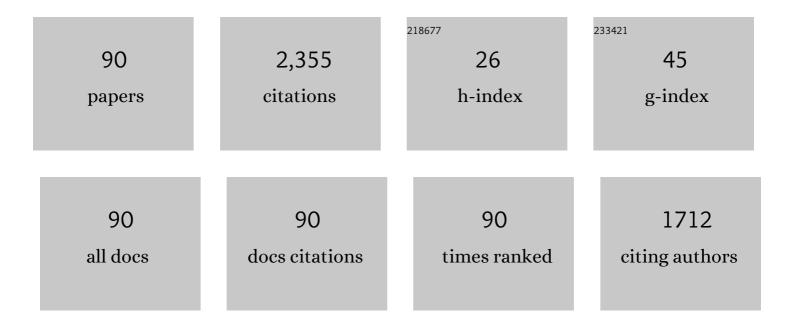
List of Publications by Year in descending order

Source: https://exaly.com/author-pdf/7110803/publications.pdf Version: 2024-02-01



#	Article	IF	CITATIONS
1	On the Electronâ€Transfer Mechanism in the Contactâ€Electrification Effect. Advanced Materials, 2018, 30, e1706790.	21.0	483
2	Raising the Working Temperature of a Triboelectric Nanogenerator by Quenching Down Electron Thermionic Emission in Contactâ€Electrification. Advanced Materials, 2018, 30, e1803968.	21.0	199
3	Contact-Electrification between Two Identical Materials: Curvature Effect. ACS Nano, 2019, 13, 2034-2041.	14.6	78
4	Effects of Metal Work Function and Contact Potential Difference on Electron Thermionic Emission in Contact Electrification. Advanced Functional Materials, 2019, 29, 1903142.	14.9	75
5	New two-layer Ruddlesden—Popper cathode materials for protonic ceramics fuel cells. Journal of Advanced Ceramics, 2021, 10, 1052-1060.	17.4	65
6	Novel Fabrication and Enhanced Photocatalytic MB Degradation of Hierarchical Porous Monoliths of MoO3 Nanoplates. Scientific Reports, 2017, 7, 1845.	3.3	64
7	Highly porous open cellular TiAl-based intermetallics fabricated by thermal explosion with space holder process. Intermetallics, 2016, 68, 95-100.	3.9	51
8	Influence of MoSi2 on oxidation protective ability of TaB2-SiC coating in oxygen-containing environments within a broad temperature range. Journal of Advanced Ceramics, 2020, 9, 703-715.	17.4	46
9	Oxidation inhibition behaviors of the HfB2-SiC-TaSi2 coating for carbon structural materials at 1700 °C. Corrosion Science, 2020, 177, 108982.	6.6	42
10	One-pot synthesis of Bi <sub>24</sub> O <sub>31</sub> Br <sub>10</sub> /Bi <sub>4</sub> V <sub>2</sub> O <sub>11</sub> heterostr and their photocatalytic properties. RSC Advances, 2014, 4, 43399-43405.	uctores	40
11	Fe-Al intermetallic foam with porosity above 60 % prepared by thermal explosion. Journal of Alloys and Compounds, 2018, 732, 443-447.	5.5	39
12	Synthesis, microstructure and properties of Ti–Al porous intermetallic compounds prepared by a thermal explosion reaction. RSC Advances, 2015, 5, 46339-46347.	3.6	36
13	Influence of the ZrB2 content on the anti-oxidation ability of ZrB2-SiC coatings in aerobic environments with broad temperature range. Journal of the European Ceramic Society, 2020, 40, 203-211.	5.7	35
14	Microstructure and high-temperature oxidation resistance of MoSi2-ZrO2 composite coatings for Niobium substrate. Journal of the European Ceramic Society, 2021, 41, 1197-1210.	5.7	35
15	Preparation of ZrB2-MoSi2 high oxygen resistant coating using nonequilibrium state powders by self-propagating high-temperature synthesis. Journal of Advanced Ceramics, 2021, 10, 1011-1024.	17.4	33
16	A stage-by-stage phase-induction and nucleation of black phosphorus from red phosphorus under low-pressure mineralization. CrystEngComm, 2017, 19, 7207-7212.	2.6	32
17	Microstructure, properties and oxidation behavior of MoSi2-MoB-ZrO2 coating for Mo substrate using spark plasma sintering. Surface and Coatings Technology, 2019, 375, 773-781.	4.8	32
18	Effect of the ZrB2 content on the oxygen blocking ability of ZrB2-SiC coating at 1973K. Journal of the European Ceramic Society, 2021, 41, 1059-1070.	5.7	32

#	Article	IF	CITATIONS
19	One-pot synthesis of Bismuth Oxyhalide/Oxygen-rich bismuth oxyhalide Heterojunction and its photocatalytic activity. Journal of Colloid and Interface Science, 2014, 431, 187-193.	9.4	31
20	Porous mullite thermal insulators from coal gangue fabricated by a starch-based foam gel-casting method. Journal of the Australian Ceramic Society, 2017, 53, 287-291.	1.9	31
21	Facile synthesis, structure and enhanced photocatalytic activity of novel BiOBr/Bi(C2O4)OH composite photocatalysts. Journal of Colloid and Interface Science, 2017, 486, 8-15.	9.4	31
22	Aluminium matrix tungsten aluminide and tungsten reinforced composites by solid-state diffusion mechanism. Scientific Reports, 2017, 7, 12391.	3.3	30
23	Microstructure and properties of Ti5Si3-based porous intermetallic compounds fabricated via combustion synthesis. Journal of Alloys and Compounds, 2014, 612, 337-342.	5.5	29
24	Dynamic oxidation protective ultrahigh temperature ceramic TaB2-20%wtSiC composite coating for carbon material. Composites Part B: Engineering, 2019, 161, 220-227.	12.0	28
25	Synthesis, microstructure and properties of MoSi 2 –5 vol%Al 2 O 3 composites. Ceramics International, 2014, 40, 16381-16387.	4.8	27
26	Synthesis and Properties of MoSi <sub>2</sub> –MoB–SiC Ceramics. Journal of the American Ceramic Society, 2016, 99, 1147-1150.	3.8	27
27	Hierarchical porous TiAl3 intermetallics synthesized by thermal explosion with a leachable space-holder material. Materials Letters, 2016, 181, 261-264.	2.6	26
28	A novel fabrication strategy for highly porous FeAl/Al2O3 composite by thermal explosion in vacuum. Vacuum, 2018, 149, 225-230.	3.5	24
29	Preparation and 1500 °C oxidation behavior of crack-free bentonite doped MoSi2 protective coating on molybdenum. Corrosion Science, 2021, 184, 109379.	6.6	24
30	Preparation of TaB 2 -SiC oxidation protective coating for carbon materials by liquid phase sintering. Ceramics International, 2018, 44, 10708-10715.	4.8	23
31	Rapid reactive synthesis of TiAl3 intermetallics by thermal explosion and its oxidation resistance at high temperature. Progress in Natural Science: Materials International, 2019, 29, 447-452.	4.4	23
32	Preparation of oxidation protective MoSi2–SiC coating on graphite using recycled waste MoSi2 by one-step spark plasma sintering method. Ceramics International, 2019, 45, 22040-22046.	4.8	22
33	Investigations of TaB2 on oxidation-inhibition property and mechanism of Si-based coatings in aerobic environment with broad temperature region for carbon materials. Journal of the European Ceramic Society, 2019, 39, 4554-4564.	5.7	22
34	Porous TiAl3 intermetallics with symmetrical graded pore-structure fabricated by leaching space holder and thermal explosion process. Intermetallics, 2018, 95, 144-149.	3.9	21
35	Reaction synthesis of spark plasma sintered MoSi2-B4C coatings for oxidation protection of Nb alloy. Ceramics International, 2019, 45, 4290-4297.	4.8	21
36	Progress of porous Al-containing intermetallics fabricated by combustion synthesis reactions: a review. Journal of Materials Science, 2021, 56, 11605-11630.	3.7	21

#	Article	IF	CITATIONS
37	Effect of high-temperature preoxidation treatment on the low-temperature oxidation behavior of a MoSi2-based composite at 500 °C. Journal of Alloys and Compounds, 2009, 473, 185-189.	5.5	20
38	Combustion synthesis of (Mo1â^'xCrx)Si2 (x=0.00–0.30) alloys in SHS mode. Advanced Powder Technology, 2012, 23, 133-138.	4.1	20
39	Reaction mechanism and oxidation resistance at 700–900 °C of high porosity NiAl intermetallic. Corrosion Science, 2021, 191, 109731.	6.6	20
40	Ultra-High Energy Storage Performance in BNT-based Ferroelectric Ceramics with Simultaneously Enhanced Polarization and Breakdown Strength. ACS Sustainable Chemistry and Engineering, 2022, 10, 9176-9183.	6.7	20
41	Effect of heating rate on porous TiAl-based intermetallics synthesized by thermal explosion. Materials and Manufacturing Processes, 2017, 32, 489-494.	4.7	19
42	Microstructure Evolution and Pore Formation Mechanism of Porous TiAl3 Intermetallics via Reactive Sintering. Acta Metallurgica Sinica (English Letters), 2018, 31, 440-448.	2.9	18
43	Exothermic behavior and thermodynamic analysis for the formation of porous TiAl3 intermetallics sintering with different heating rates. Journal of Alloys and Compounds, 2019, 811, 152056.	5.5	18
44	Complex-Shaped Porous Cu Bodies Fabricated by Freeze-Casting and Vacuum Sintering. Metals, 2015, 5, 1821-1828.	2.3	15
45	Self-propagating high temperature synthesis of MoSi2 matrix composites. Rare Metals, 2006, 25, 225-230.	7.1	14
46	Anti-oxidation modification behaviors and mechanisms of ZrB2 phase on Si-based ceramic coatings in aerobic environment with wider temperature region. Journal of Alloys and Compounds, 2018, 769, 387-396.	5.5	14
47	Multilayer Black Phosphorus Exfoliated with the Aid of Sodium Hydroxide: An Improvement in Electrochemical Energy Storage. Journal of Electronic Materials, 2018, 47, 4793-4798.	2.2	14
48	Porous NbAl3/TiAl3 intermetallic composites with controllable porosity and pore morphology prepared by two-step thermal explosion. Journal of Materials Research and Technology, 2019, 8, 3188-3197.	5.8	14
49	Significantly enhanced dielectric breakdown strength of ferroelectric energy-storage ceramics via grain size uniformity control: Phase-field simulation and experimental realization. Applied Physics Letters, 2020, 117, 212902.	3.3	14
50	Synthesis of ultraâ€fine TaB <sub>2</sub> nano powders by liquid phase method. Journal of the American Ceramic Society, 2017, 100, 5358-5362.	3.8	13
51	Preparation and highâ€ŧemperature oxidation resistance of multilayer MoSi <sub>2</sub> /MoB coating by spent MoSi <sub>2</sub> â€based materials. Journal of the American Ceramic Society, 2021, 104, 3682-3694.	3.8	13
52	Vortex domain configuration for energy-storage ferroelectric ceramics design: A phase-field simulation. Applied Physics Letters, 2021, 119, .	3.3	13
53	Fabrication and Characterization of Highly Porous FeAlâ€Based Intermetallics by Thermal Explosion Reaction. Advanced Engineering Materials, 2019, 21, 1801110.	3.5	12
54	Oxidation inhibition behaviors of HfB <sub>2</sub> â€MoSi <sub>2</sub> â€SiC oxygen blocking coating prepared by spark plasma sintering. Journal of the American Ceramic Society, 2022, 105, 1568-1580.	3.8	11

#	Article	IF	CITATIONS
55	Microstructure and properties of Al-Cr porous intermetallics fabricated by thermal explosion reaction. Materials Letters, 2018, 217, 174-176.	2.6	10
56	Oxidation Resistance of Highly Porous Fe-Al Foams Prepared by Thermal Explosion. Metallurgical and Materials Transactions A: Physical Metallurgy and Materials Science, 2018, 49, 3683-3691.	2.2	10
57	Microstructure and oxidation resistance of porous NbAl <sub>3</sub> intermetallic prepared by thermal explosion reaction. Materials Science and Technology, 2019, 35, 1624-1631.	1.6	10
58	Low temperature synthesis of pure phase TaB2 powders and its oxidation protection modification behaviors for Si-based ceramic coating in dynamic oxidation environments. Ceramics International, 2018, 44, 15517-15525.	4.8	9
59	Numerical Study on the Electron-Blocking Mechanism of Ceria-Related Composite Electrolytes Considering Mixed Conductivities of Free Electron, Oxygen Ion, and Proton. ACS Applied Energy Materials, 2019, 2, 3142-3150.	5.1	9
60	Preparation of MoSi2-SiB6 oxidation inhibition coating on graphite by spark plasma sintering method. Surface and Coatings Technology, 2021, 405, 126511.	4.8	9
61	Synthesis and hydrogenation of anatase TiO <sub>2</sub> microspheres composed of porous single crystals for significantly improved photocatalytic activity. RSC Advances, 2016, 6, 62907-62910.	3.6	8
62	Rapid Preparation of Porous Ni–Al Intermetallics by Thermal Explosion. Combustion Science and Technology, 2020, 192, 486-492.	2.3	8
63	Influence of Ta2O5 on the micromorphology and high-temperature oxidation resistance of MoSi2-based composite coating for protecting niobium. Materials Characterization, 2021, 179, 111328.	4.4	8
64	Oxidation resistance at 900°C of porous Ni-Al-Cr intermetallics synthesized via rapid thermal explosion reaction. Journal of Alloys and Compounds, 2022, 906, 164374.	5.5	8
65	Preparation of Porous NiAl Intermetallic with Controllable Shape and Pore Structure by Rapid Thermal Explosion with Space Holder. Metals and Materials International, 2021, 27, 4216-4224.	3.4	7
66	Effect of the heating rate on the thermal explosion behavior and oxidation resistance of 3D-structure porous NiAl intermetallic. Materials Characterization, 2022, 190, 112062.	4.4	7
67	Effects of Raw Materials on Synthesis, Microstructure and Properties of MoSi <sub>2</sub> -10 Vol% SiC Composites. Transactions of the Indian Ceramic Society, 2016, 75, 33-39.	1.0	6
68	Fabrication of Highly Porous CuAl Intermetallic by Thermal Explosion Using NaCl Space Holder. Jom, 2018, 70, 2173-2178.	1.9	6
69	Recycling Molybdenum Oxides from Waste Molybdenum Disilicides: Oxidation Experimental Study and Photocatalytic Properties. Oxidation of Metals, 2019, 92, 1-12.	2.1	6
70	Interfacial microstructure and mechanical properties of Ti/Cu joint manufactured by Ni-Al thermal explosion reaction. Journal of Manufacturing Processes, 2020, 57, 919-929.	5.9	6
71	Visible Observation and Formation Mechanism of Porous TiAl3 Intermetallics During the Continuous Sintering Process. Jom, 2020, 72, 3652-3660.	1.9	6
72	Effects of Oxygen Vacancies and Cation Valence States on the Triboelectric Property of Substoichiometric Oxide Films. ACS Applied Materials & Interfaces, 2021, 13, 35795-35803.	8.0	6

#	Article	IF	CITATIONS
73	Recycling MoSi2 heating elements for preparing oxidation resistant multilayered coatings. Journal of the European Ceramic Society, 2022, 42, 921-934.	5.7	6
74	Fabrication of highly porous TiAl3 intermetallics using titanium hydride as a reactant in the thermal explosion reaction. Journal of Materials Research, 2018, 33, 2680-2688.	2.6	5
75	Preparation and moderate temperature oxidation behavior of Ti- and Al-doped NbSi2-Si3N4 composite coatings on Nb alloy. Surface and Coatings Technology, 2019, 379, 125005.	4.8	5
76	Amorphous Iron Boride in Situ Grown on Black Phosphorus Sheets: A Promising Electrocatalyst for OER. Journal of Electronic Materials, 2022, 51, 3705-3713.	2.2	5
77	Pore formation mechanism and oxidation resistance of porous CoAl3 intermetallic prepared by rapid thermal explosion. Intermetallics, 2022, 147, 107592.	3.9	5
78	Combustion synthesis and mechanical properties of MoSi <sub>2</sub> –ZrB <sub>2</sub> –SiC ceramics. Journal of the Ceramic Society of Japan, 2018, 126, 504-509.	1.1	4
79	<i>In situ</i> growth of porous carbon with adjustable morphology on black phosphorus nanosheets for boosting electrocatalytic H <sub>2</sub> and O <sub>2</sub> evolution. New Journal of Chemistry, 2021, 45, 12203-12212.	2.8	4
80	Effect of film-forming regulation of the self-formed compound layer on the oxidation inhibition capacity of HfB2-SiC coating. Ceramics International, 2022, 48, 22039-22052.	4.8	4
81	Reversal of triboelectric charges on sol–gel oxide films annealed at different temperatures. Applied Physics Letters, 2021, 118, .	3.3	3
82	One-step synthesis via solution combustion of Fe(III)-doped BiOCl nanoparticles with high photocatalytic activity. Journal of Sol-Gel Science and Technology, 2022, 103, 309-318.	2.4	3
83	Oxidation of TaB2-SiC coatings prepared by spark plasma sintering and effect of pre-oxidation treatments. Journal of the European Ceramic Society, 2022, 42, 5238-5248.	5.7	3
84	Fabrication and Characterization of (Mo <sub>1â€<i>x</i></sub> Ni <sub><i>x</i></sub> ) (Si <sub>1â€<i>x</i></sub> Al <sub><i>x</i></sub> ) <sub>2</sub> ( <i>x</i> = 0.025, 0.05, and 0.1) Alloys. International Journal of Applied Ceramic Technology, 2016, 13, 359-366.	2.1	2
85	Solvothermal synthesis of weakly crystalline cobalt–nickel sulfide to obtain high pseudocapacitance. Journal of Materials Science: Materials in Electronics, 2021, 32, 11072-11083.	2.2	2
86	A sandwich structure of cobalt pyrophosphate/nickel phosphite@C: one step synthesis and its good electrocatalytic performance. Journal of Solid State Electrochemistry, 2022, 26, 1221-1230.	2.5	2
87	Dissimilar Metal Joining of Ti and Ni Using Ti-Al Powder Interlayer Via Rapid Thermal Explosion Method. Journal of Materials Engineering and Performance, 2020, 29, 7239-7249.	2.5	1
88	Microstructural Characterization and Antiâ€Oxidation Properties of Molybdenum Disilicide Coating on Niobium by Spent MoSi <sub>2</sub> â€Based Materials. Advanced Engineering Materials, 2021, 23, .	3.5	1
89	Oxygen barrier capability of ZrB2-SiC coating at 1700°C strengthened by film-forming treatment. Corrosion Science, 2022, 205, 110456.	6.6	1
90	Microstructure and properties of Co–Al porous intermetallics fabricated by thermal explosion reaction. High Temperature Materials and Processes, 2021, 40, 141-150.	1.4	0